Energy attenuated by Ni powder distribution during laser cladding on Cu-Ni-Al substrate

F Bourahima, T Baudin, M Rege, V Ji, F Brisset, A L Helbert

Energy attenuated by Ni powder distribution during laser cladding on Cu-Ni-Al substrate

F. Bourahima[1,2*], T. Baudin[2], M. Rege[1], V. Ji[2], F. Brisset[2], A.L. Helbert[2]

[1] Etablissements Chpolansky, 3 Rue Angiboust, 91 462 Marcoussis

[2] ICMMO, SP2M, Université Paris-Saclay, UMR CNRS 8182, bât.410, 91405 ORSAY, France

Abstract

Laser metal deposition (LMD) is an alternative method to other cladding techniques such as Plasma Transfer Arc (PTA) or blowtorch for surface treatment in the glass industry. It aims to produce dense, high-quality coatings on a non-planar surface without affecting its thermal and mechanical properties. In this study, Ni based coatings were coated onto Cu-Ni-Al substrate using a 3 JET nozzle technique. During laser cladding, good metallurgical bonding is necessary to ensure the further surfacing process technique. A microstructural analysis was conducted, and the mechanical properties were then evaluated with microhardness analysis to link process parameters to coating bonding quality. A calculation of the power attenuation attempts to explain the impact of the powder distribution on the bonding.

This work revealed that a chemical dilution zone exists between coating and substrate and is necessary for perfect metallurgical bonding. The heterogeneous bonding, observed through the section, along the curved interface coating/substrate, has been linked to the Gaussian distribution of the powder that attenuates the input power. The attenuated powder was measured all along the interface.

Keywords: Laser cladding, Power attenuation, Powder distribution, Dilution zone

*** Corresponding author:**

BOURAHIMA Fazati ; Tel: +33 (0) 1 69 80 15 27 ; E-mail: fazati.bourahima@chpolansky.fr

1 Introduction

During bottle production, viscous glass is poured into Cu-Ni-Al molds at temperatures ranging from 700 to 1200°C. A glass mold must absorb the high glass temperature in order to cool it homogeneously. However, during this process, corrosion or even abrasion can appear on sensitive parts of the molds. Therefore, it is important to modify the mold surface properties in order to extend its lifespan.

Laser cladding is an innovative surfacing technique [1] used to obtain well-bonded high-quality materials, free of pores and cracks without affecting the substrate thermal properties. Many studies have investigated the Heat Affected Zone (HAZ), which is a zone belonging to the substrate that has not reached its fusion temperature *but observed a change in its structure due to the process. In the mold industry, the aim is to limit this zone in order to prevent changes in the base material thermal properties. Currently, the main techniques used are Plasma Transferred Arc (PTA) and blowtorch. But these techniques create a very high HAZ.

Some researchers have investigated the impact of laser cladding on the substrate microstructural change. In most of the studies, the HAZ is observed during laser cladding on cast iron substrates with the appearance of metastable phases like martensite or ledeburite [2-6]. Arabi Jeshvaghani *et al*. [3] have added that sometimes a complete graphite dissolution can be observed in the case of cladding on cast iron with spheroidal graphite. In some cases, this HAZ can lead to cracking behavior [3].

Balu *et al*. [7] have operated laser cladding with two kinds of Ni based powder on Cu substrate with and without pre-heating. They observed that the grain size in the HAZ is greater than it is further away from the interface. It has also been seen that this size increases at low laser scanning speed. Hardness is lower in the HAZ than it is further away from the interface. They found that a pre-heating of the substrate leads to a better bonding due to a larger melting pool and HAZ.

Despite the limited HAZ, laser cladding often induces an area of local chemical dilution between the powder and the substrate. Authors have explained that in order to obtain dilution, a fusion

between the substrate and the coating has to be present [7][8][9]. This dilution, dependent on the input laser [10], has to be restricted in order to avoid a large HAZ but seems necessary to ensure good metallurgical bonding. There are two ways of describing the dilution (rate) [11]: in geometrical terms, which consists in calculating the ratio between the melted area (including the HAZ) and the coating area. The second is in metallurgical terms, which consists in measuring the depth of the chemical mixture between the coating and the substrate. Liu *et al*. [12] present a dilution rate by using the geometrical method during laser cladding of magnesium alloys. According to them, a too low dilution rate prevents good metallurgical bonding. Using the same definition of the dilution rate, Luo *et al*. [13] present the same observation during laser cladding of NiCrBSi. Balu *et al*. [7] used the metallurgical method to measure the dilution rate during laser cladding of Ni based powder on a Cu substrate. They found that a high dilution can lead to a high HAZ. Pereira *et al*. [14] observed during laser cladding of NiCoCrBSi on stainless steel, that a very low dilution zone (metallurgical method) at about 2 μm is enough to obtain a perfect bonding without affecting the mechanical properties of the substrate (no cracking behavior observed). O.S. Adesina *et al*. [15] presented an EDS analysis to measure the dilution between two materials and chemical evolution of the materials' components [16].

The main challenge in laser cladding on a copper-based substrate is to obtain good bonding despite the low absorptivity of the substrate. Zhang *et al*. [17] explained that it was impossible to obtain bonding without preheating, so they pre-heated the substrate to 300°C.

In the mold industry, the HAZ must be limited in order to avoid changing the molds' thermal properties and thus obtain a homogeneous glass surface. It appears that a compromise must be found to respect both the restricted HAZ and the dilution zone needed to guarantee the cohesion between the coating and the substrate. We should bear in mind that this cohesion is crucial to allow further machining of the repaired mold. Moreover, the clad has to be free of cracks and pores to retain a perfect glass surface.

The aim of this study is to obtain perfect bonding with a limited or non-existent HAZ. This can be achieved by identifying the relationship between the dilution zone (existence and thickness) and the bonding quality between coating and substrate with regards to the laser process parameters. The laser cladding of Ni powder on a Cu based substrate will be performed without preheating and on a curved surface. A microstructural and chemical analysis of the coating/substrate interface will be conducted. Also, microhardness measurements will be presented. The influence of the Gaussian distribution of Ni powder on the laser power attenuation, and thus on the bonding, will be discussed.

2 Materials and experimental techniques

Laser cladding consists in melting an injected powder with a very thin surface layer of the substrate by a laser beam to produce a metallurgical bonding. During this study, a 4KW Nd: YAG laser with a wavelength of 1030 nm was used. An optical fiber with a diameter of 600 µm was used for guiding the beam. Ni powder was injected coaxially into the laser beam. A cross section of the Cu-Ni-Al mold of the bottle ring is shown in Figure 1a after cladding. Figure 1b describes the typical cross section that has been metallurgically studied.

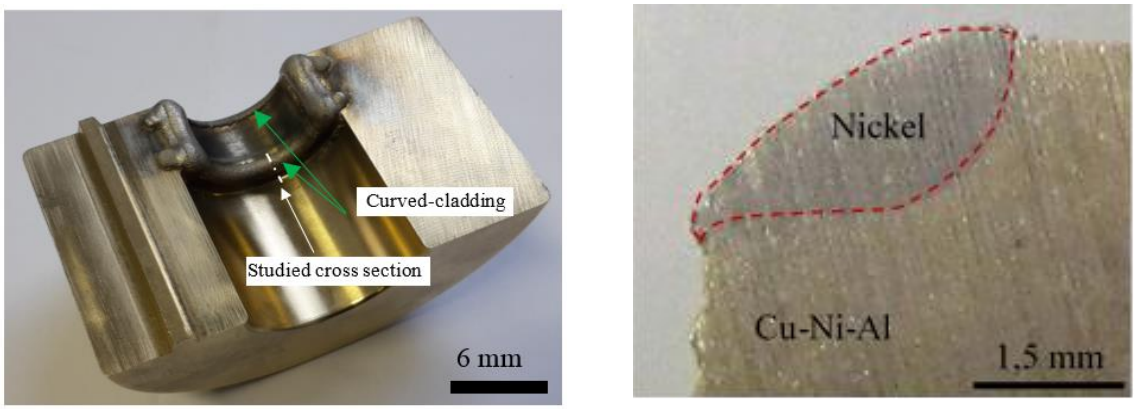

Figure 1: a) Half of the mold ring after Ni-laser cladding and b) studied cross section

During the process, the interaction distance, *fs*, between the laser and the powder is considered (Figure 2):

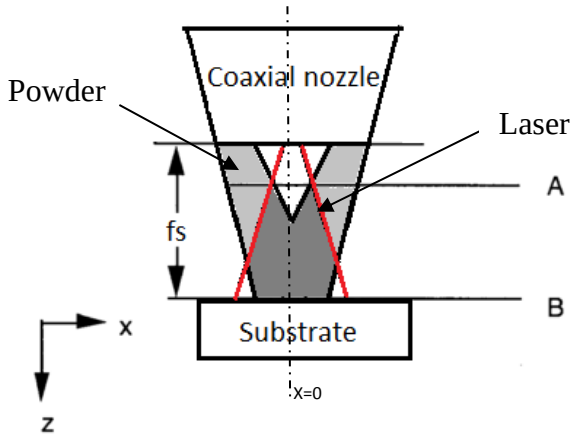

Figure 2: Powder distribution according to the focal position fs [18]

At the focal plane (position B), the powder flow follows a Gaussian distribution. This has been proved by many research studies [18-20]. In the present study, the Gaussian distribution has been centered at the midpoint of the mold curved surfaces of the samples.

The chemical compositions of the powder and the substrate are listed in Table 1.

Table 1: Chemical compositions of the substrate and powder

Elements (wt%)	Fe	Mn	Al	Ni	Zn	Pb	Sn	Si	Cu	B	Cr	C
Cu-Ni-Al	<1	0.5	8.5	15	8	<0.1	0.15	1	Bal	-	-	-
Ni powder	1	0.1	-	Bal	-	-	-	2.5	-	1.7	0.3	0.5

The process parameters used during this study are presented in Table 2. These samples are extracted using Taguchi design of experiment. Only samples with a partial or perfect bonding have been selected.

Table 2 : Process parameters

Sample	Power (W)	Speed (mm/s)	Powder Feeding Rate (g/min)	Spot diameter (mm)
CNC 1	2400	6.5	26.5 g/mm	4 mm
CNC 2	2600	10	24.5 g/mm	3 mm
CNC 3	2800	6.5	32.5 g/mm	3 mm
CNC 4	2800	8.5	24.5 g/mm	4 mm
CNC 5	3200	8.5	28.5 g/mm	3 mm
CNC 6	3200	10	30.5 g/mm	4 mm

To be characterized, samples were mechanically polished using SiC papers and then diamond polished to 1 µm for Optical Microscopy (OM), Scanning Electron Microscopy (SEM) and Energy Dispersive Spectroscopy (EDS) analyses. To operate Electron Backscatter Diffraction (EBSD), an extra OPS polishing was done. Vickers hardness tests were performed on the cross section, along a line perpendicular to the coating surface with a 10-gf load for 15 seconds. The measurements were taken from either side of the interface for all the 6 samples.

3 Results and discussion

3.1 Microstructure features and associated chemical and mechanical properties

Figure 3 describes the three different kinds of bonding behavior that can be observed: perfect bonding (Figure 3a), partial bonding (Figure 3b) where the bonding is partially present at the interface and no bonding (Figure 3c).

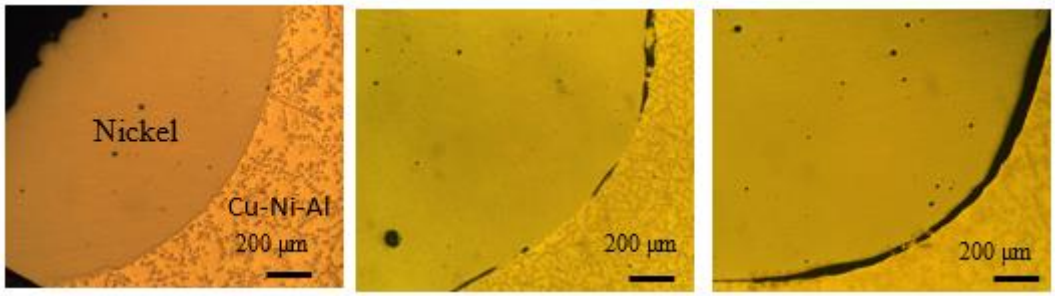

Figure 3: Three kinds of bonding behavior a) perfect bonding b) partial bonding and c) no bonding

Figure 4 shows the SEM-BSE (Back-Scattered Electrons) analysis of the CNC 5 and CNC 6 samples (see Table 2). Figure 4a shows that CNC 5 presents perfect bonding (case of Figure 3a) whereas Figure 4b shows a sample (CNC 6) with a discontinuous bonding (Figure 3b). Indeed, in the center of the curve, there is a lack of bonding. No analyses have been performed on samples with no bonding (Figure 3c) since the clad is easily separated from the substrate.

For both samples, the substrate is composed of a dendritic matrix. No heat affected zone (HAZ) seems to be present in the substrate because no microstructure modification is noticeable close to the interface with the clad. Concerning the Ni deposit, elongated grains are observed along solidification direction for both cases. Small grains can be seen close to the interface and at the extreme coating surface.

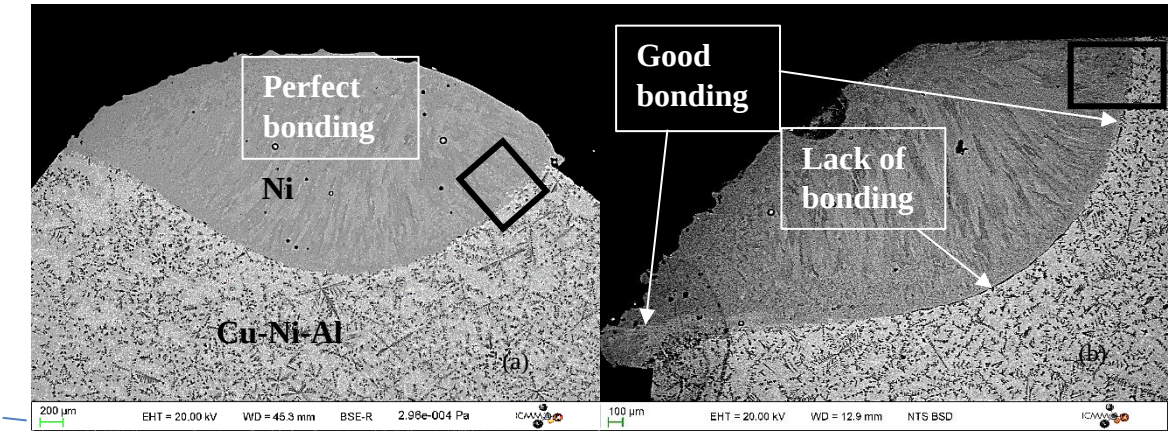

Figure 4: Typical microstructure of the cross section of the samples a) CNC 5 with good bonding, b) CNC 6 with partial bonding obtained by SEM-BSE

Figure 5 shows an EBSD analysis of the microstructure and texture around the interface (black squares in 4a and b) for both samples (perfect or partial bonding) in order to observe the differences due to the bonding quality.

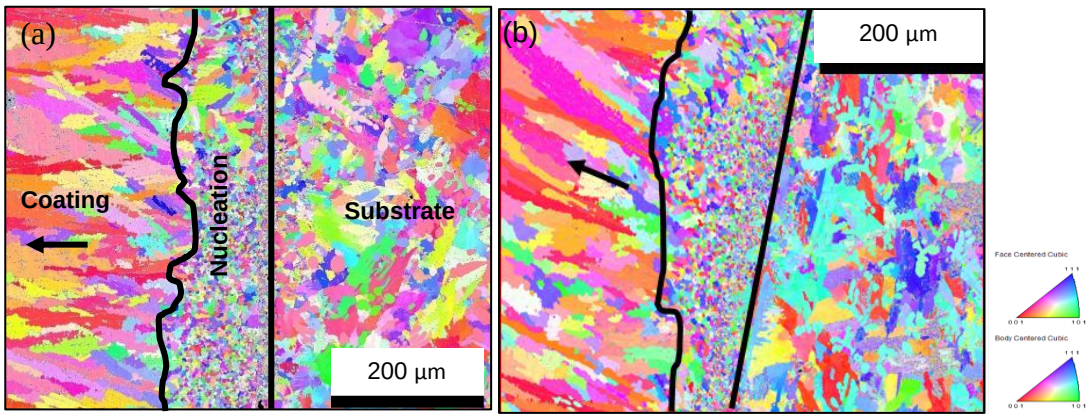

Figure 5: Crystallographic axes parallel to the solidification direction (black arrows). a) EBSD analysis of the black square area in Figure 4a and b) in Figure 4b.

It can be observed that microstructure is very similar in both cases (Figure 5a and 5b).

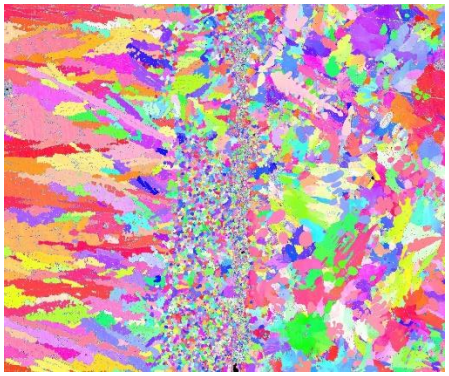

The solidification features are in accordance with the literature [21-24]. A nucleation phase, characterized by small equiaxed grains, is evidenced at the interface, then a columnar growth directed mainly parallel to the <001> direction of the dendrites is observed (Figure 5a).

A SEM-EDS analysis is presented (Figure 6) to observe the chemical impact of the laser cladding at the interface nucleation/substrate.

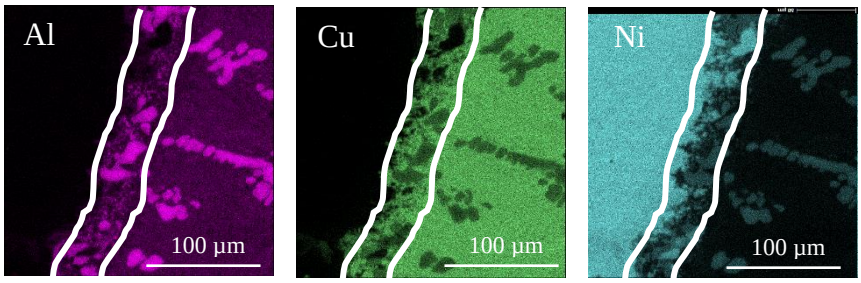

(a) (b) (c)

Figure 6: EDS maps of the principal chemical elements composing the deposit and the substrate of sample CNC6 (a) Al, (b) Cu, (c) Ni

Figure 6 clearly shows a local chemical mixture at the interface coating/substrate delimited by white lines where copper seems to be replaced by nickel over a thin layer of the substrate. This can be the consequence of a local fusion of the substrate and correspond to the dilution zone that has been reported in the literature [17] [25]. Apart from this area, there are no discernible chemical changes in the substrate or the Ni coating. So, no HAZ can be chemically observed in this study.

A measurement of the dilution zone thickness was made by chemical analysis from the coating to the substrate (Figure 7).

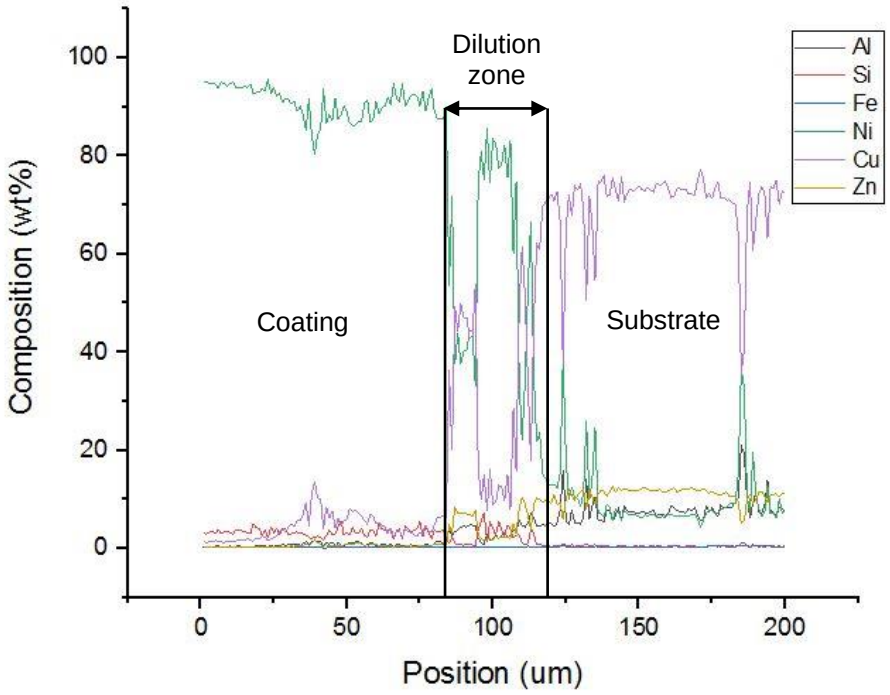

Figure 7: Chemical composition of the dilution zone from the coating to the substrate (sample CNC 6)

A diminution of the Ni element from the coating to the substrate can be observed. At the same time, the Cu composition progressively increases. Overall, Ni is at around 96% in the coating, then decreases down to 40% close to the interface and stays below 10% in the substrate matrix except inside the dendrites where the Ni increases to 39%. The dendrites also present a higher level of Al (the high concentration of Ni and Al inside the dendrites is in accordance with Figure 6). The dilution zone exhibits a chemical mixture over about 35µm for this sample.

Figure 8 shows the hardness measurements through the interface for four typical features of the microstructure: the columnar zone of the coating, the nucleation zone, the dilution zone and the substrate.

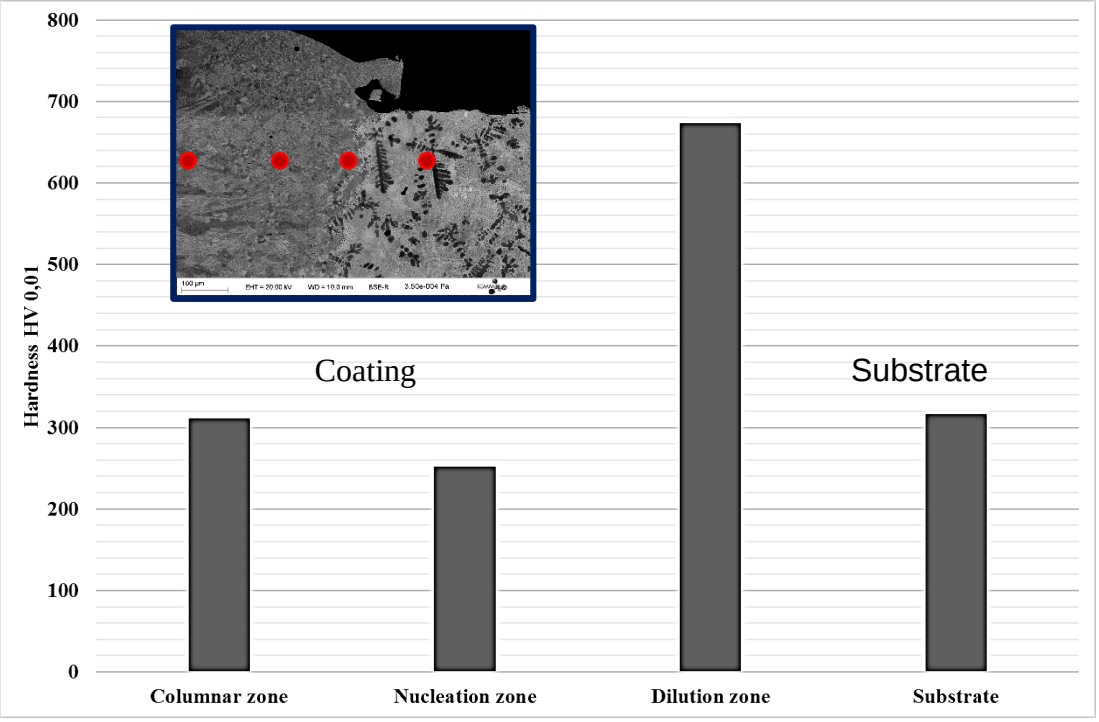

Figure 8: Hardness measurements corresponding to the characteristic features encountered from the coating to the substrate (red points)

It can be observed from Figure 8 that the micro-hardness of the dilution zone increased to 618 HV compared to the coating and the substrate which are not higher than 317 HV. The high hardness in the dilution zone could be explained by the formation of an eutectic of Ni-Ni_3B due to the low ratio of Si/B (≈1.3) in this area as shown by Hemmatie *et al*. [26]. Indeed, they mention that this compound is of high hardness. No increase of hardness is noticed in the nucleation area despite the presence of small grains.

Since the dilution zone can be quantified using the EDS analysis it could be interesting to observe its evolution along the curved interface in order to corroborate its existence/thickness with the metallurgical bonding quality.

3.2 Dilution zone thickness along the curved interface

In order to state if the discontinuous bonding along the interface in the studied section is linked to the chemical dilution presence or thickness, a protocol of systematic DZ quantification has been implemented across the section of all samples and is presented in Figure 9. Five lines separated from each other by an angle of 22.5° along which the chemical composition have been measured from the

coating to the substrate within 400 µm, and where the DZ depth has been determined. Thanks to this method, it is possible to plot the DZ evolution along the curved interface (Figure 9).

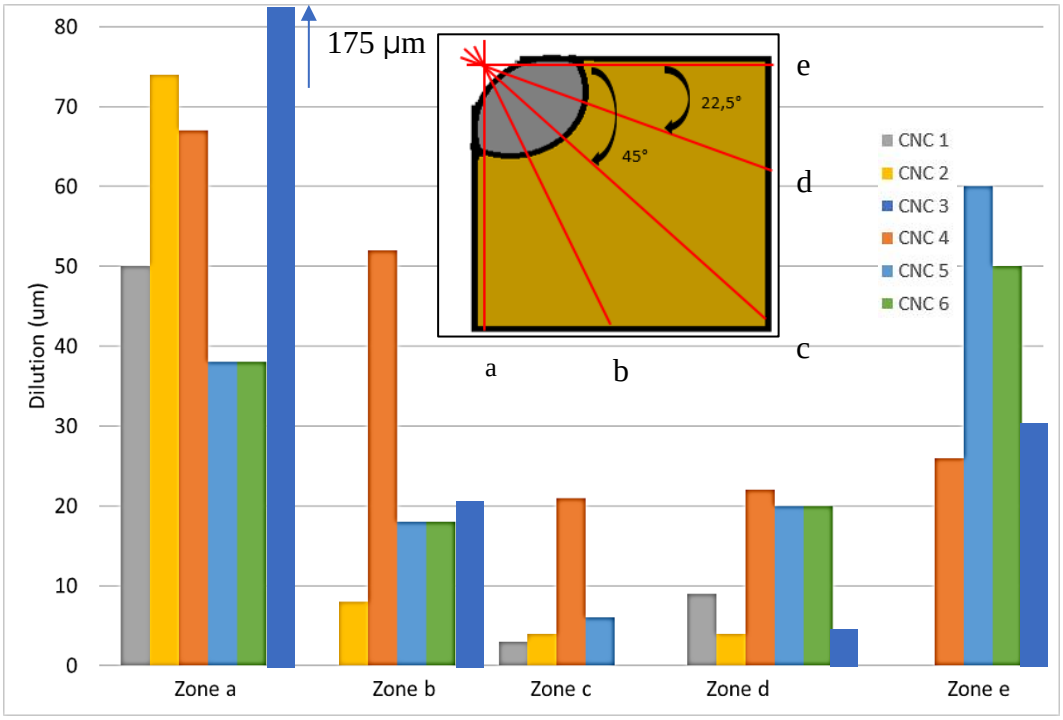

Figure 9: Measurement of the DZ depth over the entire cross section and DZ depth along the five red lines for all the samples

Figure 9 reveals that the DZ evolution is the same across the section for all the samples studied. On the zones a and e (the edges), the DZ depth is maximum (from 25 to 175 µm). It decreases at lower levels (b and d zones) to between 3 and 21 µm. Then at the center of the curve (c zone) this DZ is minimum (zero in the case of no bonding at all). Moreover, for all the samples studied, the bonding is lower at the center of the curve section. Therefore, it is possible to draw a direct connection between DZ depth and bonding quality. Indeed, the deeper the DZ, the better the bonding will be. The discontinuous bonding is well highlighted by the DZ evolution along the curve of the cross section. We would attempt to consider what phenomenon leads systematically to a weaker chemical dilution at the curve center of the section during laser cladding, regardless of process parameters.

3.3 Power attenuation

It is well known in the laser cladding process that powder particles contribute to attenuate the incident laser power. Tabernero *et al*. [27] have described the impact of a shadow of particles during

the interaction of the laser and the powder while cladding is in progress. They have assessed the attenuation undergone by the beam and characterized the density of energy that reaches the surface of the substrate. They were able to perform this calculation with a computational fluid dynamics (CFD) model, which has been experimentally validated. Moreover, the present authors used the calculation of the attenuated power to determine the minimum power necessary to ensure an accurate clad/substrate bonding [25]. Nevertheless, the local attenuation due to the Gaussian powder distribution has not been studied along the curve section.

El Cheikh *et al*. [19] have discovered that at the focal position, fs, presented in Figure 2, a Gaussian distribution of powder can be observed. Qi *et al*. [28] have proposed an equation of the powder distribution $N(x,z)$ depending on the radial distance x and the axial distance z in the case of a coaxial nozzle as shown:

$$N(x,z) = N_{max}(z).Exp(-2x^2/R^2) \quad (1)$$

With $N_{max}[m^{-3}]$ the peak concentration at the center of powder flow (x=0), x[mm] the radial distance and R[mm] the powder stream.

To understand how the power is impacted, the Beer Lambert Law can be applied [28][29]:

$$P'_z(x,z) = P_z(x).Exp(-\alpha SNz) \quad (2)$$

With $P'_z[W]$ the power attenuated by the powder flow, $P_z[W]$ the initial input power during laser cladding, S $[mm^2]$ the particle section and α a factor which considers phenomena like the scattering effect, plasma generation... α was obtained from an experiment of the attenuated power during laser cladding. A power meter is placed under an optically neutral glass to protect it from the powder injected. During the test, an air flow was injected horizontally in order to deflect the projected powder. As an example, for an incident measured power of 1916 W, the measured attenuated power was 1498 W for a PFR of 28.5 g/min. This led to adjusting the α coefficient at a value of 6 (this result is in accordance with literature [27]). If α is equal to 1, the attenuation is only due to particle shadow. The present value of 6 indicates that other phenomena (scattering effect, plasma generation...) also contribute to the power attenuation.

By inputting the powder distribution on each position of x it is possible to observe the power attenuation on the radial distance for an incident power of 2800W as an example (Figure 10).

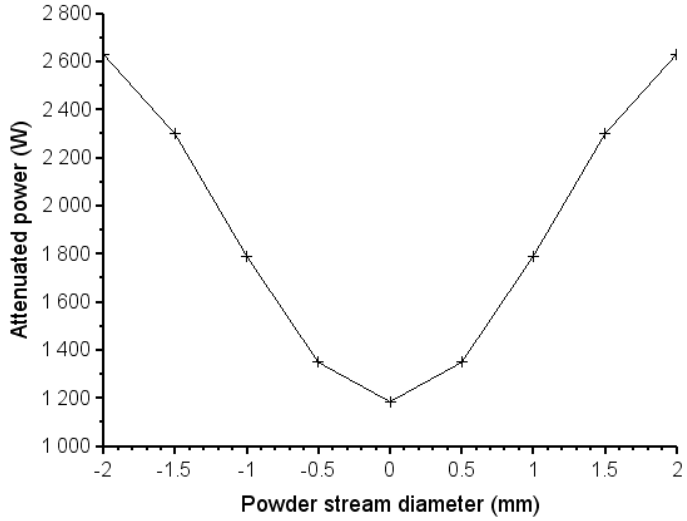

Figure 10: Distribution of the power attenuation on the substrate (x=0 is the focal point) for an input laser power of 2800 W

Figure 10 indicates that, at the center of the powder flow (at the focal point fs Figure 2) the power is attenuated from 2800 to 1200W. At the center of the powder flow (x=0), 57% of the power is lost due to the powder flow (absorbed or reflected). So, only 43% is available for the fusion. Moreover, given that the absorptivity of Cu based materials is about 0.06, only 72W remains to reach the substrate (and probably melt it). Since the focal plane of the powder flow corresponds to the center of the mold curved surface, it can be assumed that this shadow effect explains the lack of dilution DZ observed at this position of the section. Therefore, this phenomenon may be at the origin of the absence of bonding for some cladding conditions with too weak incident laser power.

4 Conclusion

Ni based powder was deposited by laser cladding on a Cu based substrate with a curved surface. The cladding process parameters were widely explored in order to verify the bonding quality of the clad to the substrate. Three kinds of metallurgical bonding have been noted: lack of bonding, partial bonding or perfect bonding. In addition, a constant lack of bonding is observed in the center of the substrate curved surface. Moreover, the chemical dilution depth between Ni and Cu was

measured at the interface clad/substrate depending on process parameters. It appears that the dilution depth is also lower at the same location of the curved surface. This could be explained by the Gaussian distribution of the powder flow around this point. Indeed, at the curved center the powder density is at maximum, so the input laser power is significantly attenuated. Less energy is then available for the substrate to melt and to ensure a perfect metallurgical bonding. The attenuated power evolution moving away from this central point would explain the discontinuous bonding along the interface in the cross section.

Acknowledgments

The authors wish to thank C. Aboud, N. Barbosa and C. Lafarge from the ETS CHPOLANSKY for their help in the sample elaboration by laser cladding and their great skill in the field of this technology applied to non-planar surfaces. This research was supported by the ANRT (French National Agency for Research and Technology) and ETS Chpolansky.

References

[1] W.M. Steen, J. Mazumder, Laser Material Processing, 4th ed., Springer, 2010.

[2] F. Bourahima, A.L. Helbert, V. Ji, M. Rege, A. Courteaux, F. Brisset, T. Baudin, Optimization of Microstructural Evolution during Laser Cladding of Ni Based Powder on GCI Glass Molds, Key Eng. Mater. 813 (2019) 185–190.

[3] H. Liu, J. Hao, Z. Han, G. Yu, X. He, H. Yang, Microstructural evolution and bonding characteristic in multi-layer laser cladding of NiCoCr alloy on compacted graphite cast iron, J. Mater. Process. Technol. 232 (2016) 153–164.

[4] R. Arabi Jeshvaghani, M. Jaberzadeh, H. Zohdi, M. Shamanian, Microstructural study and wear behavior of ductile iron surface alloyed by Inconel 617, Mater. Des. 54 (2014) 491–497.

[5] C.M. Lin, W.Y. Kai, C.Y. Su, K.H. Key, Empirical alloys-by-design theory calculations to the microstructure evolution mechanical properties of Mo-doped laser cladding NiAl composite coatings on medium carbon steel substrates, J. Alloys Compd. 702 (2017) 679–686.

[6] Y. Liu, X. Zhan, P. Yi, T. Liu, B. Liu, Q. Wu, Research on the transformation mechanism of graphite phase and microstructure in the heated region of gray cast iron by laser cladding, Opt. Laser Technol. 100 (2018) 79–86.

[7] P. Balu, E. Rea, J. Deng, Laser cladding of nickel-based alloy coatings on copper substrates, Proc. SPIE. 9657 (2015) 1–10.

[8] S. Saqib, R.J. Urbanic, K. Aggarwal, Analysis of laser cladding bead morphology for developing additive manufacturing travel paths, Procedia CIRP. 17 (2014) 824–829.

[9] Y.F. Tao, J. Li, Y.H. Lv, L.F. Hu, Effect of heat treatment on residual stress and wear behaviors of the TiNi/Ti2Ni based laser cladding composite coatings, Opt. Laser Technol. 97 (2017) 379–389.

[10] C.K. Kim, S.G. Choi, J.H. Kim, H.J. Jo, Y.C. Jo, S. pil Choi, Y.T. Cho, Characterization of

surface modification by laser cladding using low melting point metal, J. Ind. Eng. Chem. 87 (2020) 54–59.

[11] E. Toyserkani, K. Amir, C. Stephen, Laser Cladding, CRC PRESS, 2006.

[12] J. Liu, H. Yu, C. Chen, F. Weng, J. Dai, Research and development status of laser cladding on magnesium alloys: A review, Opt. Lasers Eng. 93 (2017) 195–210.

[13] X. Luo, J. Li, G.J. Li, Effect of NiCrBSi content on microstructural evolution, cracking susceptibility and wear behaviors of laser cladding WC/Ni-NiCrBSi composite coatings, J. Alloys Compd. 626 (2015) 102–111.

[14] J.C. Pereira, J.C. Zambrano, E. Rayón, A. Yañez, V. Amigó, Mechanical and microstructural characterization of MCrAlY coatings produced by laser cladding: The influence of the Ni, Co and Al content, Surf. Coatings Technol. 338 (2018) 22–31.

[15] O.S. Adesina, B.A. Obadele, G.A. Farotade, D.A. Isadare, A.A. Adediran, P.P. Ikubanni, Influence of phase composition and microstructure on corrosion behavior of laser based Ti–Co–Ni ternary coatings on Ti–6Al–4V alloy, J. Alloys Compd. 827 (2020) 1–11.

[16] S. Wang, C. Liu, Real-time monitoring of chemical composition in nickel-based laser cladding layer by emission spectroscopy analysis, Materials (Basel). 12 (2019) 1–15.

[17] Y. Zhang, Y. Tu, M. Xi, L. Shi, Characterization on laser clad nickel based alloy coating on pure copper, Surf. Coatings Technol. 202 (2008) 5924–5928.

[18] E. Ferreira, M. Dal, C. Colin, G. Marion, C. Gorny, D. Courapied, J. Guy, P. Peyre, Experimental and numerical analysis of gas/powder flow for different LMD nozzles, Metals (Basel). 10 (2020) 1–20.

[19] H. El Cheikh, B. Courant, S. Branchu, J.Y. Hascoët, R. Guillén, Analysis and prediction of single laser tracks geometrical characteristics in coaxial laser cladding process, Opt. Lasers Eng. 50 (2012) 413–422.

[20] S. Pouzet, P. Peyre, C. Gorny, O. Castelnau, T. Baudin, F. Brisset, C. Colin, P. Gadaud, Additive layer manufacturing of titanium matrix composites using the direct metal deposition

laser process, Mater. Sci. Eng. A. 677 (2016) 171–181.

[21] B. Song, T. Yu, X. Jiang, W. Xi, X. Lin, The relationship between convection mechanism and solidification structure of the iron-based molten pool in metal laser direct deposition, Int. J. Mech. Sci. 165 (2020) 1-14

[22] P. Peyre, V. Vignal, Traitements de surface par laser et tenue à la corrosion aqueuse, Tech. l'ingénieur. COR1580 (2012) 1–12.

[23] J. Philibert, A. Vignes, Y. Bréchet, P. Combrade, La solidification des métaux et des alliages, in: MASSON (Ed.), Métallurgie Du Minerai Au Matériau, MASSON, 1998: pp. 555–573.

[24] T. DebRoy, H.L. Wei, J.S. Zuback, T. Mukherjee, J.W. Elmer, J.O. Milewski, A.M. Beese, A. Wilson-Heid, A. De, W. Zhang, Additive manufacturing of metallic components – Process, structure and properties, Prog. Mater. Sci. 92 (2018) 112–224.

[25] J.C. Pereira, J.C. Zambrano, M.J. Tobar, A. Yañez, V. Amigó, High temperature oxidation behavior of laser cladding MCrAlY coatings on austenitic stainless steel, Surf. Coatings Technol. 270 (2015) 243–248.

[26] I. Hemmati, V. Ocelík, J.T.M. De Hosson, Effects of the alloy composition on phase constitution and properties of laser deposited Ni-Cr-B-Si coatings, Phys. Procedia. 41 (2013) 302–311.

[27] I. Tabernero, A. Lamikiz, S. Martínez, E. Ukar, L.N. López De Lacalle, Modelling of energy attenuation due to powder flow-laser beam interaction during laser cladding process, J. Mater. Process. Technol. 212 (2012) 516–522.

[28] H. Qi, J. Mazumder, H. Ki, Numerical simulation of heat transfer and fluid flow in coaxial laser cladding process for direct metal deposition, J. Appl. Phys. 100 (2006) 1–11.

[29] P. Peyre, P. Aubry, R. Fabbro, R. Neveu, A. Longuet, Analytical and numerical modelling of the direct metal deposition laser process, J. Phys. D. Appl. Phys. 41 (2008) 1–10.

Tables caption

Figures caption

For the **Table of Contents** of the issue :

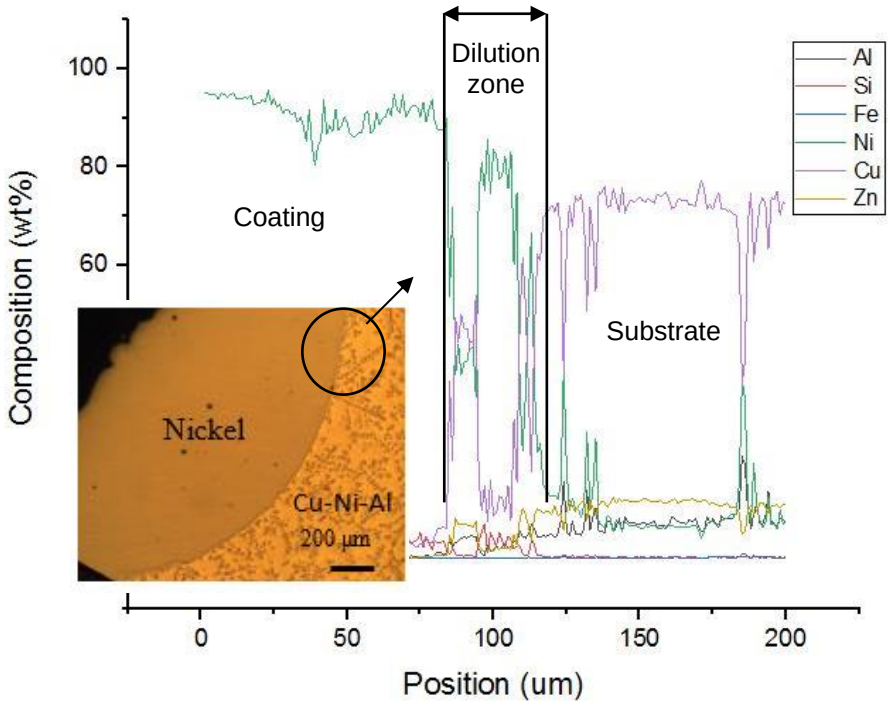

Heterogeneous bonding, linked to chemical dilution depth, is observed between coating and substrate after laser cladding of Ni based powder on a Cu-Ni-Al glassmold curved surface. Bonding defect has been related to the gaussian distribution of the Ni powder. Indeed, the Ni particles attenuate the input laser power and may prevent the substrate melting that ensures the metallurgical bonding.